JCI The Journal of Clinical Investigation

P2X7 receptor signaling contributes to tissue factor–dependent thrombosis in mice

Christian Furlan-Freguia, … , Zaverio M. Ruggeri, Wolfram Ruf

J Clin Invest. 2011;121(7):2932-2944. https://doi.org/10.1172/JCI46129.

Research Article **Hematology**

Thrombosis is initiated by tissue factor (TF), a coagulation cofactor/receptor expressed in the vessel wall, on myeloid cells, and on microparticles (MPs) with variable procoagulant activity. However, the molecular pathways that generate prothrombotic TF in vivo are poorly defined. The oxidoreductase protein disulfide isomerase (PDI) is thought to be involved in the activation of TF. Here, we found that in mouse myeloid cells, ATP-triggered signaling through purinergic receptor P2X, ligand-gated ion channel, 7 (P2X7 receptor; encoded by *P2rx7*) induced activation (decryption) of TF procoagulant activity and promoted release of TF^+ MPs from macrophages and SMCs. The generation of prothrombotic MPs required P2X7 receptor–dependent production of ROS leading to increased availability of solvent-accessible extracellular thiols. An antibody to PDI with antithrombotic activity in vivo attenuated the release of procoagulant MPs. In addition, $P2rx7^{-/-}$ mice were protected from TF-dependent $FeCl_3$-induced carotid artery thrombosis. BM chimeras revealed that P2X7 receptor prothrombotic function was present in both hematopoietic and vessel wall compartments. In contrast, an alternative anti-PDI antibody showed activities consistent with cellular activation typically induced by P2X7 receptor signaling. This anti-PDI antibody restored TF-dependent thrombosis in $P2rx7^{-/-}$ mice. These data suggest that PDI regulates a critical P2X7 receptor–dependent signaling pathway that generates prothrombotic TF, defining a link between inflammation and thrombosis with potential implications for antithrombotic therapy.

P2X7 receptor signaling contributes to tissue factor–dependent thrombosis in mice

Christian Furlan-Freguia,[1] Patrizia Marchese,[2] András Gruber,[3] Zaverio M. Ruggeri,[2] and Wolfram Ruf[1]

[1]Department of Immunology and Microbial Science, and [2]Department of Molecular and Experimental Medicine, The Scripps Research Institute, La Jolla, California, USA. [3]Department of Biomedical Engineering and Department of Medicine, Oregon Health and Sciences University, Portland, Oregon, USA.

Thrombosis is initiated by tissue factor (TF), a coagulation cofactor/receptor expressed in the vessel wall, on myeloid cells, and on microparticles (MPs) with variable procoagulant activity. However, the molecular pathways that generate prothrombotic TF in vivo are poorly defined. The oxidoreductase protein disulfide isomerase (PDI) is thought to be involved in the activation of TF. Here, we found that in mouse myeloid cells, ATP-triggered signaling through purinergic receptor P2X, ligand-gated ion channel, 7 (P2X7 receptor; encoded by *P2rx7*) induced activation (decryption) of TF procoagulant activity and promoted release of TF$^+$ MPs from macrophages and SMCs. The generation of prothrombotic MPs required P2X7 receptor–dependent production of ROS leading to increased availability of solvent-accessible extracellular thiols. An antibody to PDI with antithrombotic activity in vivo attenuated the release of procoagulant MPs. In addition, *P2rx7*$^{-/-}$ mice were protected from TF-dependent $FeCl_3$-induced carotid artery thrombosis. BM chimeras revealed that P2X7 receptor prothrombotic function was present in both hematopoietic and vessel wall compartments. In contrast, an alternative anti-PDI antibody showed activities consistent with cellular activation typically induced by P2X7 receptor signaling. This anti-PDI antibody restored TF-dependent thrombosis in *P2rx7*$^{-/-}$ mice. These data suggest that PDI regulates a critical P2X7 receptor–dependent signaling pathway that generates prothrombotic TF, defining a link between inflammation and thrombosis with potential implications for antithrombotic therapy.

Introduction

In the current view of thrombus formation, exposure of tissue factor (TF) in the injured vessel wall is a crucial event that initiates thrombosis in high-flow vessels, such as the carotid artery (1, 2). In vitro studies demonstrate that TF procoagulant activity is tightly regulated, and TF is switched from a cryptic, nonactive state to a decrypted, active state by a number of cellular agonists or manipulations (3), but the mechanisms of TF decryption and the relevance of these in vitro findings for thrombosis remain a matter of ongoing debate (4–10). The cell surface TF procoagulant activity is regulated by chaperones, subcellular localization, and possibly dimerization and glycosylation (11–16) and is enhanced by the exposure of procoagulant phosphatidylserine (PS) (3). However, PS exposure alone cannot explain the decryption of TF in all cellular models (8, 9, 17).

Protein disulfide isomerase–dependent (PDI-dependent) redox regulation of TF's extracellular allosteric Cys^{186}-Cys^{209} disulfide bond was proposed as an alternative mechanism that directly alters macromolecular substrate recognition required for coagulation, while preserving the cell signaling function of TF (7, 8). PDI is an oxidoreductase localized mainly in the endoplasmic reticulum (ER), but on the cell surface, PDI is crucial for protein S-nitrosylation and nitric oxide uptake (18, 19). PDI may influence TF procoagulant function through thiol- and nitric oxide–dependent mechanisms, since TF is susceptible to S-nitrosylation and glutathionation (7, 20, 21). Antibody inhibition of PDI has antithrombotic effects in mice (21, 22), and it was proposed that PDI released from injured cells activates cryptic TF on microparticles (MPs) (21).

Myeloid cells represent a source for circulating MPs, and the generation and targeting of these MPs to thrombi is dependent on the interaction between P-selectin and P-selectin glycoprotein ligand–1 (PSGL-1) (23–27). Although stimulation of purinergic receptor P2X, ligand-gated ion channel, 7 (P2X7 receptor; encoded by *P2rx7* in mice), by ATP has been shown to release TF$^+$ MPs from dendritic cells of potential relevance for immune responses or sepsis (28), the mechanisms that generate prothrombotic TF$^+$ MPs are poorly understood. The P2X7 receptor is expressed on myeloid and vascular cells (29). P2X7 receptor is essential for maturation and release of IL-1β (30) and is unique among the ATP-gated channels for its ability to open transiently a membrane pore permeable to high–molecular weight dyes involving pannexin-1 hemichannel-dependent and -independent mechanisms (31–34). The P2X7 receptor is further connected to integrins and stimulates cytoskeletal rearrangements (35).

In the present study, we showed that the P2X7 receptor is crucial for TF activation and release on MPs carrying integrin β1, PSGL-1, and PDI from myeloid cells as well as for the release of procoagulant MPs from SMCs. TF-dependent thrombosis was reduced in *P2rx7*$^{-/-}$ mice, and P2X7 receptor signaling in hematopoietic and vessel wall cells supported thrombosis. Our findings delineate what we believe to be a novel role for thiol pathways as critical regulators of procoagulant TF$^+$ MP generation downstream of P2X7 receptor signaling.

Results

ATP stimulation of the P2X7 receptor decrypts TF activity on macrophages. TF procoagulant activity was investigated in BM-derived macrophages primed with interferon-γ and LPS to induce TF expression (36). Cell surface TF activity on intact cells was found to be very low and required activation, e.g., with ionomycin (3), that was thiol-dependent and poorly correlated with

Conflict of interest: The authors have declared that no conflict of interest exists.
Citation for this article: *J Clin Invest.* 2011;121(7):2932–2944. doi:10.1172/JCI46129.

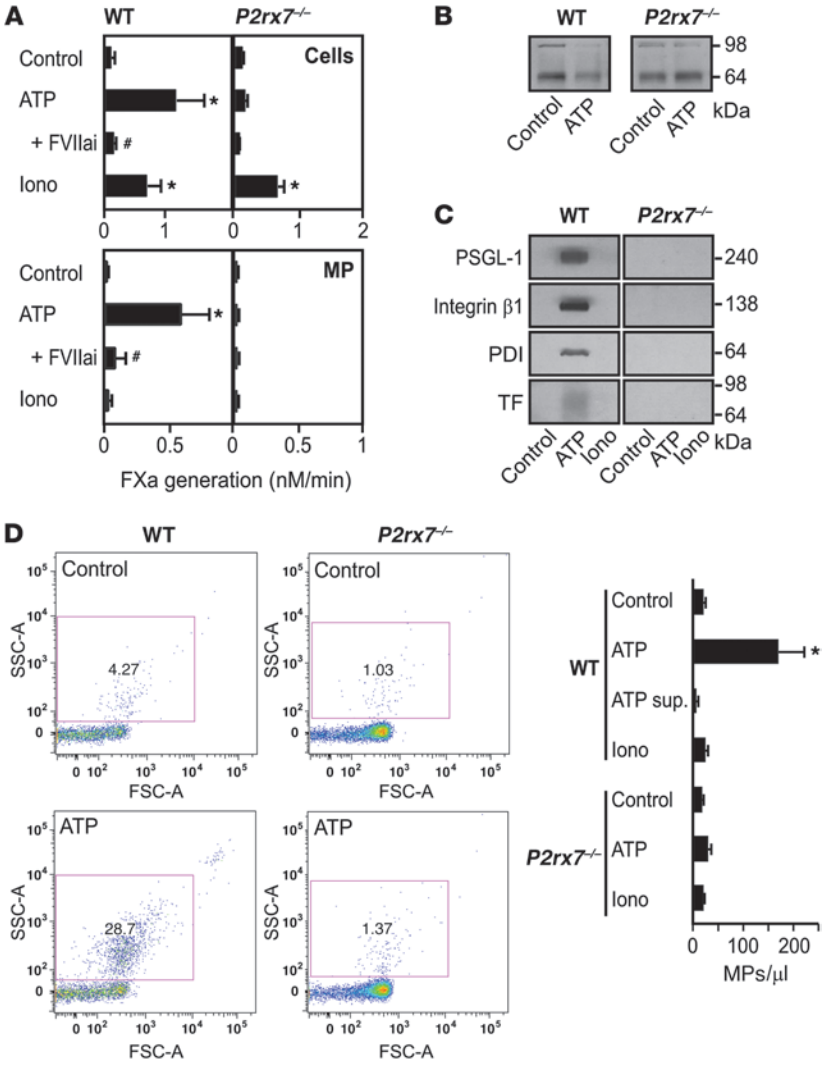

Figure 1
ATP activation of P2X7 receptor induces macrophage TF activation coupled to TF+ MP release. (**A**) TF activity, measured by FXa generation assays on macrophage cell surfaces or released MPs after stimulation with ATP (5 mM) or ionomycin (10 μM). FVIIai (100 nM) was used to demonstrate TF specificity ($n \geq 4$). *$P < 0.01$ vs. control; #$P < 0.01$ vs. ATP. (**B**) Western blotting for TF in WT or *P2rx7*$^{-/-}$ macrophages before and after stimulation with 5 mM ATP for 30 minutes; blots are representative of at least 3 independent experiments. (**C**) Western blotting for MP-associated proteins; blots are representative of at least 4 independent experiments. (**D**) FACS analysis of MPs released from ATP stimulated macrophages. ATP sup., supernatants of ATP-stimulated cells after MP depletion by centrifugation. Shown are typical plots of MP detection on a LSR-II flow cytometer and quantitation of particle counts from 2–3 experiments performed in triplicate; *$P < 0.001$ vs. control.

the surface exposure of PS (Supplemental Figure 1; supplemental material available online with this article; doi:10.1172/JCI46129DS1). Although ionomycin is not a physiological agonist, cell injury generates high concentrations of extracellular ATP that activates P2X7 receptor signaling known to induce TF (*f3*) mRNA expression in monocytes (37) and the release of TF+ MPs from dendritic cells (28). ATP induced TF decryption on primed macrophages (Figure 1A). Control experiments using modification of crucial Lys residues required for TF procoagulant activity (38) showed that encrypted TF was predominantly surface exposed prior to activation (Supplemental Figure 2).

The time course of cellular TF activation — normalized for TF expression, assessed by Western blotting — showed that ionomycin maximally induced TF activity after 5 minutes, whereas ATP continued to increase activity, reaching 10-fold higher levels relative to ionomycin-stimulated cells after 30 minutes (Supplemental Figure 3). As further indication of the distinct activation mechanisms by the 2 agonists, stimulation with ATP, but not ionomycin, generated procoagulant MPs after 30 minutes (Figure 1A). Calcium ionophores such as ionomycin have been used to generate procoagulant MPs from myeloid cells. In control experiments, we found that MP release was enhanced by the addition of extracellular Ca^{2+}. Under these conditions, ionomycin promoted the release of procoagulant MPs, albeit with 3-fold lower efficiency compared with ATP. Using our standard conditions, ATP-stimulated MP procoagulant activity was confirmed to be TF dependent by blockade with active site–inhibited factor VIIa (FVIIai; Figure 1A). Monoclonal antibody 21E10, generated in the laboratory against murine TF, also inhibited MP procoagulant activity by greater than 70%.

Neither TF activation nor procoagulant MP release occurred after ATP stimulation of macrophages from *P2rx7*$^{-/-}$ mice. Ionomycin induced TF cell surface activation normally in *P2rx7*$^{-/-}$ macrophages, and Western blotting for TF demonstrated that P2X7 receptor was not necessary for TF synthesis in primed macrophages (Figure 1B). A substantial fraction of cellular TF was lost after 30 minutes of ATP stimulation of WT macrophages, but not *P2rx7*$^{-/-}$ macrophages, excluding the possibility that ATP markedly induced TF synthesis in WT macrophages during the short incubation period.

ATP activation of macrophages promoted the release of MPs that carried TF, the thrombus-targeting receptor PSGL-1 (23, 24, 27), integrin β1, and PDI (Figure 1C). Determination of MP abundance by flow cytometry showed that 30 minutes of stimulation with ATP promoted a 9-fold increase in MP numbers above baseline (Figure 1D). Specificity of the signal was confirmed by

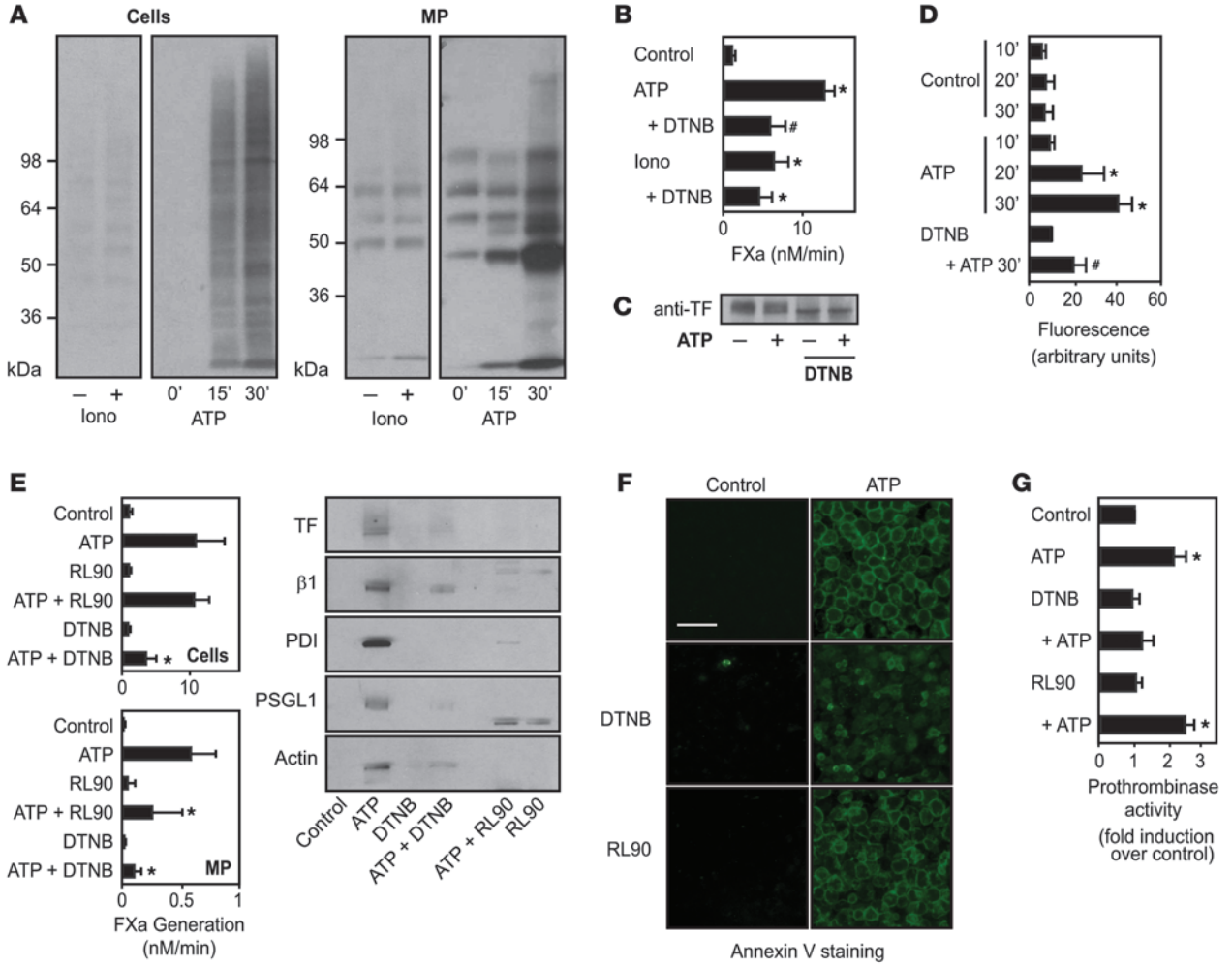

Figure 2

Role of free thiols and PDI in ATP-dependent TF$^+$ MP release. (**A**) ATP, but not ionomycin, induced exposure of solvent-accessible free thiols on the macrophage cell surface and MPs in a time-dependent manner. Free thiols were labeled with MPB (100 μM) and visualized by streptavidin-HRP. Blots are representative of 4 independent experiments. (**B**) Thiols were blocked with 2 mM DTNB prior to 30-minute stimulation with ionomycin or ATP ($n = 3$). $^*P < 0.004$ vs. control, $^{\#}P < 0.001$ vs. ATP alone. (**C**) DTNB's effect on TF electrophoretic mobility after 30 minutes with or without ATP; blots are representative of 3 independent experiments. (**D**) MP release, quantified using membrane labeling with NBD (3 μM) of ATP-stimulated cells with or without DTNB (3 independent experiments). $^*P < 0.004$ vs. control; $^{\#}P < 0.01$ vs. ATP alone. (**E**) RL90 (10–20 μg/ml) and DTNB (2 mM) inhibited release of MPs and procoagulant activity; DTNB, but not RL90, also inhibited TF activation on cell surfaces ($n \geq 4$). $^*P < 0.01$ vs. ATP alone. Note that Western blots for integrin β1 and PSGL-1 showed cross-reactivity of the detection antibody with RL90 present in the samples. Blots are representative of 3 independent experiments. (**F**) Effect of DTNB (2 mM) and RL90 on macrophage PS exposure, with or without ATP (5 mM). Scale bar: 500 μm. (**G**) Prothrombinase activity of WT macrophages with 30-minute ATP stimulation with or without DTNB and RL90 ($n = 3$). $^*P < 0.02$ vs. control.

analysis of supernatants that were depleted of MPs by centrifugation, and no increased release was seen upon stimulation of *P2rx7*$^{-/-}$ cells. Thus, under these experimental conditions, baseline spontaneous MP release was low, and P2X7 receptor signaling promoted release of increased numbers of MPs carrying the proteome signature shown in Figure 1C.

ATP stimulation of P2X7 receptor induces thiol- and PDI-dependent release of TF$^+$ MPs. Prompted by the finding that PDI was released on MPs, we addressed potential roles of thiol exchange in TF$^+$ MP release by labeling extracellular free thiols with membrane-impermeable N-(3-maleimidopropionyl)-biocytin (MPB) that was added during the stimulation. Only ATP activation of P2X7 receptor, not stimulation by ionomycin, induced the appearance of solvent-accessible free thiols on cells. Although free thiols were detected on MPs released at baseline, ATP increased the release of thiol-labeled MPs (Figure 2A). The maleimide compound might have simply trapped reaction intermediates, but labeling of cell-free supernatants after the release reaction similarly detected free thiols in MP proteins. Furthermore, in the presented experiments, the labeling reaction was typically quenched with an excess of reduced Cys prior to the recovery of MPs, excluding the possibility that free thiols became accessible as an artifact of the MP isolation procedure. These data raised the question of whether PDI-dependent thiol exchange pathways regulated MP release downstream of P2X7 receptor signaling.

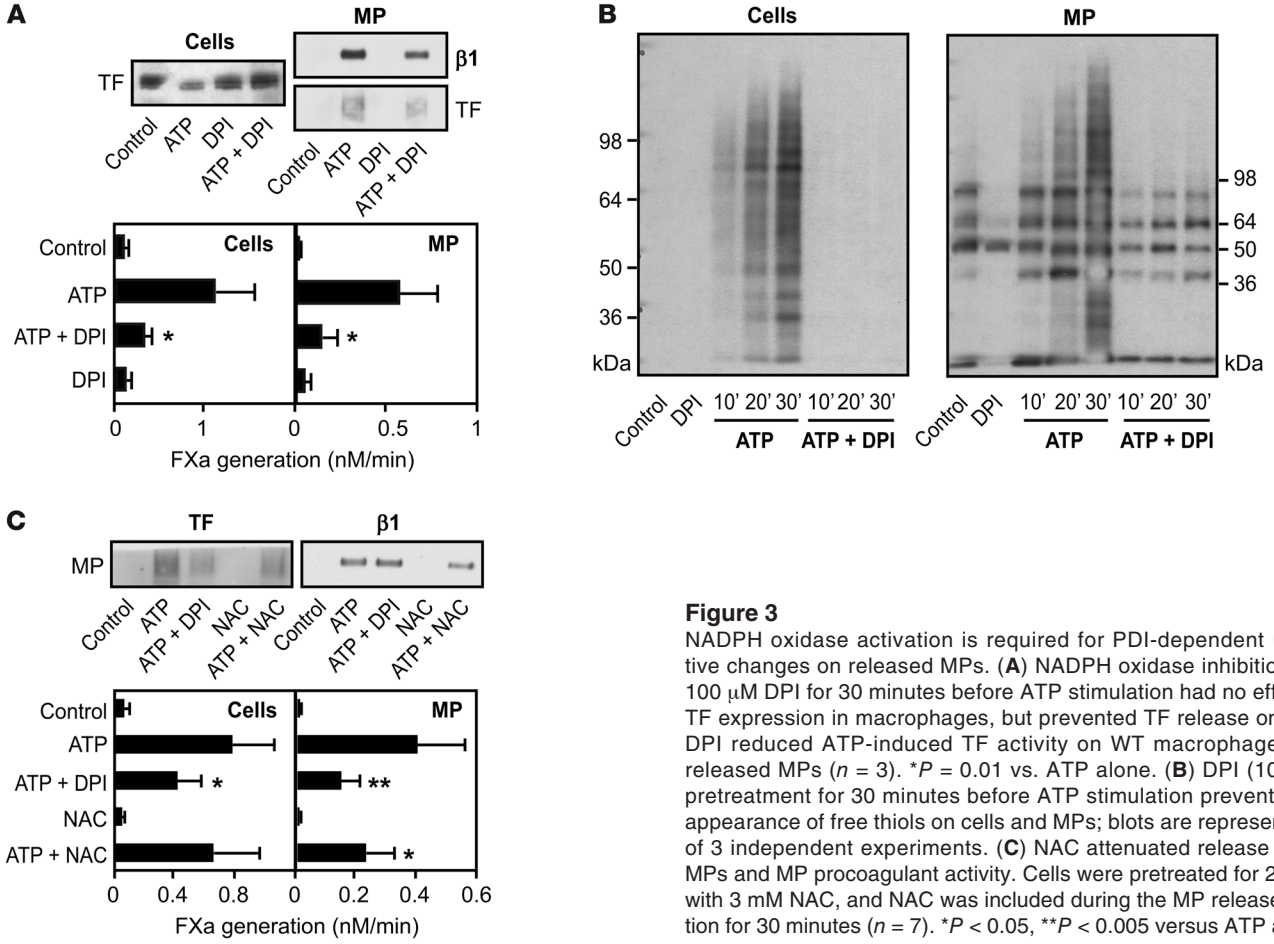

Figure 3
NADPH oxidase activation is required for PDI-dependent reductive changes on released MPs. (**A**) NADPH oxidase inhibition with 100 μM DPI for 30 minutes before ATP stimulation had no effect on TF expression in macrophages, but prevented TF release on MPs. DPI reduced ATP-induced TF activity on WT macrophages and released MPs (n = 3). *P = 0.01 vs. ATP alone. (**B**) DPI (100 μM) pretreatment for 30 minutes before ATP stimulation prevented the appearance of free thiols on cells and MPs; blots are representative of 3 independent experiments. (**C**) NAC attenuated release of TF$^+$ MPs and MP procoagulant activity. Cells were pretreated for 2 hours with 3 mM NAC, and NAC was included during the MP release reaction for 30 minutes (n = 7). *P < 0.05, **P < 0.005 versus ATP alone.

Prolonged stimulation with ATP continued to increase TF procoagulant activity on cells (Supplemental Figure 3). The delayed increase of TF activity was blocked by reacting solvent-accessible free thiols with dithio-bis-2-nitrobenzoic-acid (DTNB; Figure 2B). Western blotting of TF in DTNB-treated cells showed that DTNB altered the electrophoretic mobility of cellular TF (Figure 2C), which indicates that TF was a potential target for thiol-dependent modifications. Release of MPs was directly quantified by membrane labeling with the fluorescent dye 6-([N-{7-nitrobenz-2-oxa-1,3-diazol-4-yl}amino]hexanoyl)sphingosyl phosphocholine (NBD) (39). ATP produced a time-dependent increase of MPs released over baseline, and MP release was attenuated significantly in DTNB-treated cells (Figure 2D). Quantification of ATP-induced MP release by FACS also showed a significant reduction in the presence of DTNB (control, 9.8- ± 4.2-fold over baseline; DNTB, 2.3- ± 0.5-fold over baseline; P < 0.001). P2X7 receptor signaling also triggers the release of the proinflammatory cytokine IL-1β. The appearance of processed IL-1β in the supernatant of stimulated macrophages was reduced in the presence of DTNB (Supplemental Figure 4). Taken together, these data showed that blockade of free thiols inhibited the P2X7 receptor–dependent release of inflammatory cytokines and MPs.

Although the anti-PDI antibody RL90, with antithrombotic activity in vivo (21, 22), did not attenuate ATP-induced cell surface TF activity, it significantly reduced the release of MP procoagulant activity, similar to DTNB (Figure 2E). Both DTNB and RL90 attenuated the release of TF, PDI, integrin β1, actin, and PSGL1 on MPs, which demonstrated that MPs carrying this signature proteome were generated by a thiol-dependent pathway. Neither DTNB nor RL90 had an effect on baseline PS exposure or the known exteriorization of PS by ATP (40), although the PS staining appeared to be more apical in DNTB-treated versus ATP-stimulated cells (Figure 2F), presumably reflecting differences in cell morphology. In addition, DTNB, but not RL90, attenuated prothrombinase activity on ATP-stimulated cells (Figure 2G). Since both DTNB and RL90 blocked MP release, cell surface exposure of procoagulant PS was not sufficient to induce the release of MPs. Taken together, these data demonstrated a critical role of thiol pathways for the generation of TF-bearing, procoagulant MPs and identified blockade of TF$^+$ MP release as a potential novel mechanism for the antithrombotic effects of RL90 (21, 22).

TF activation and TF$^+$ MP generation are dependent on ROS generation. Since RL90 significantly reduced the release of MPs carrying solvent-accessible free thiols (Supplemental Figure 5), inhibition of PDI's reductase function represented a plausible mechanism for the inhibition of thiol-dependent MP release by the antibody. However, P2X7 receptor activation induces protein denitrosylation (41), and RL90 also blocks the denitrosylase activity of PDI (19, 42), providing an alternative explanation for the appearance of extracellular free thiols after ATP stimulation. P2X7 receptor signaling activates NADPH oxidases to generate ROS that scavenge nitric oxide released from S-nitrosylated proteins (41). ROS inhibi-

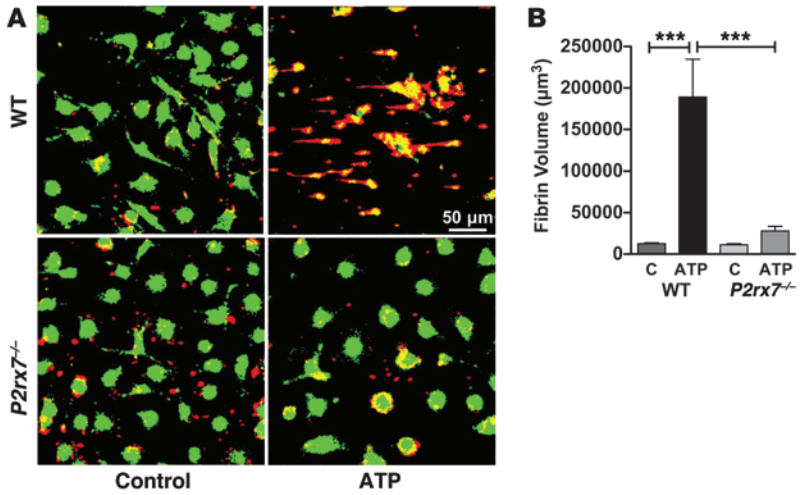

Figure 4
Fibrin deposition onto surface-adherent mouse macrophages perfused with mouse blood. (**A**) Visualization of WT and *P2rx7*$^{-/-}$ unstimulated and ATP-stimulated macrophages with deposited fibrin after blood perfusion (see Methods). Images are superpositions of corresponding green (cells) and red (fibrin) fluorescence images binarized after application of a threshold to eliminate background fluorescence; yellow denotes colocalization. Only isolated single platelets and small aggregates adhered to the cell surface or to matrix between cells. (**B**) Volume of deposited fibrin (see Methods). Data are mean ± SEM from 3 independent experiments. ***$P < 0.001$, ANOVA followed by Bonferroni multiple-comparison test.

tors such as N-acetyl cysteine (NAC) and the flavoenzyme inhibitor diphenyleneiodonium (DPI), but not inhibitors of nitric oxide synthases, block these downstream effects of P2X7 receptor signaling.

While nitric oxide synthase inhibitors were without effect (data not shown), a 30-minute pretreatment with DPI did not change macrophage TF levels, but prevented the typical loss of TF from ATP-stimulated cells and reduced the release of TF on MPs (Figure 3A). In addition, ATP stimulation of TF cell surface activity and the release of procoagulant MPs were reduced. Thiol labeling of DPI-pretreated cells showed that solvent-accessible free thiols were no longer exposed on cells, and DPI inhibited released MP thiols to baseline levels (Figure 3B). These data implicate ROS generation, presumably through nitric oxide scavenging, as a crucial step in promoting MP release after ATP stimulation. As an independent line of evidence, cells were pretreated for 120 minutes with the ROS scavenger NAC (Figure 3C). The results further supported the critical importance of ROS generation for the P2X7 receptor–dependent generation of prothrombotic TF$^+$ MPs.

Macrophage prothrombotic activity is dependent on P2X7 receptor activation in whole blood under flow. In order to exclude the possibility that the observed requirement for P2X7 receptor–dependent TF decryption was a peculiar effect of the chosen experimental conditions, we studied fibrin formation on macrophage cell surfaces in whole blood under flow. As shown in Figure 4, fibrin formation on untreated cells was minimal; in contrast, ATP stimulation of WT macrophages, but not *P2rx7*$^{-/-}$ macrophages, resulted in abundant fibrin deposition covering cells that remained attached to the surface and extended as strands elongated in the direction of flow. These data supported the conclusion that macrophage TF remains encrypted under quasiphysiological conditions of flowing blood and demonstrated that P2X7 receptor activation is a sufficient stimulus to trigger myeloid cell prothrombotic activity.

P2X7 receptor deficiency protects mice from thrombosis in vivo. The physiological relevance of the P2X7 receptor–dependent TF activation pathway for hemostasis and thrombosis was studied in *P2rx7*$^{-/-}$ mice, which carry a signaling-disabling deletion in the P2X7 receptor cytoplasmic domain (43). Tail bleeding was used as the model to detect potential defects in hemostasis. Blood loss after clipping of the 2-mm-diameter tail tip did not reveal hemostatic impairment in *P2rx7*$^{-/-}$ mice (WT, 1.0 ± 0.4 OD_{575nm}; *P2rx7*$^{-/-}$, 0.9 ± 0.4 OD_{575nm}; $n = 7$).

Contributions of P2X7 receptor to thrombosis were studied in the $FeCl_3$ injury model of the carotid artery. Challenge with the commonly used dose of 8% $FeCl_3 \cdot 6H_2O$ (0.30 M Fe^{3+}) caused stable occlusion in C57BL/6 mice, whereas *P2rx7*$^{-/-}$ mice were significantly protected from thrombosis (Figure 5A). However, injury induced by a higher 10% $FeCl_3 \cdot 6H_2O$ dose (0.37 M Fe^{3+}) elicited carotid artery occlusion that was not significantly different between *P2rx7*$^{-/-}$ and WT mice (Figure 5A). These contrasting results prompted further evaluation of TF's contribution to thrombogenesis in response to arterial injury caused by different Fe^{3+} concentrations. Consistent with the previous demonstration that the intrinsic pathway also plays an important role in determining vascular occlusion (44), we found that a 125–250 ng/g body weight dose of the anti–factor XI (anti-FXI) monoclonal antibody 14E11 (45) always prevented carotid artery thrombosis after 8% or 10% $FeCl_3 \cdot 6H_2O$ injury in WT mice. A dose of 62 ng/g of the same antibody was noninhibitory in WT mice, but significantly prevented carotid artery occlusion after 10% $FeCl_3 \cdot 6H_2O$ injury in *P2rx7*$^{-/-}$ mice (Figure 5A), which suggests that attenuated TF procoagulant function in the latter renders thrombus formation more susceptible to inhibition of the contact phase of coagulation. Injection of anti-mouse TF antibody 21E10 failed to reduce thrombosis in both WT and *P2rx7*$^{-/-}$ mice at 10% $FeCl_3 \cdot 6H_2O$ (Figure 5A).

The difficulty of inhibiting TF procoagulant function in blood has been previously documented with most antibodies used (46); consequently, this pharmacologic approach leads to only partial TF blockade compared with genetic deletion. We confirmed this with anti-TF 21E10 injected at 25 μg/g before 8% $FeCl_3 \cdot 6H_2O$ carotid artery injury; however, the same dose prevented vascular occlusion in the presence of the 62 ng/g anti-FXI 14E11 dose that was not inhibitory when administered alone (Figure 5B). This result and the above data in *P2rx7*$^{-/-}$ mice support the validity of probing alterations of TF procoagulant function by attenuating the contact phase pathway that contributes to thrombogenesis in the $FeCl_3$ arterial injury model. Using this approach, we evaluated whether PDI plays a functional role in TF-dependent thrombosis. Previous studies in nonocclusive arterial injury models showed that blocking PDI with RL90 attenuated fibrin deposition (21, 22). Accordingly, in WT mice challenged with 8% $FeCl_3 \cdot 6H_2O$, anti-PDI RL90 dose-dependently prevented vascular occlusion when coadministered with the noninhibitory dose of anti-FXI 14E11 (Figure 5B).

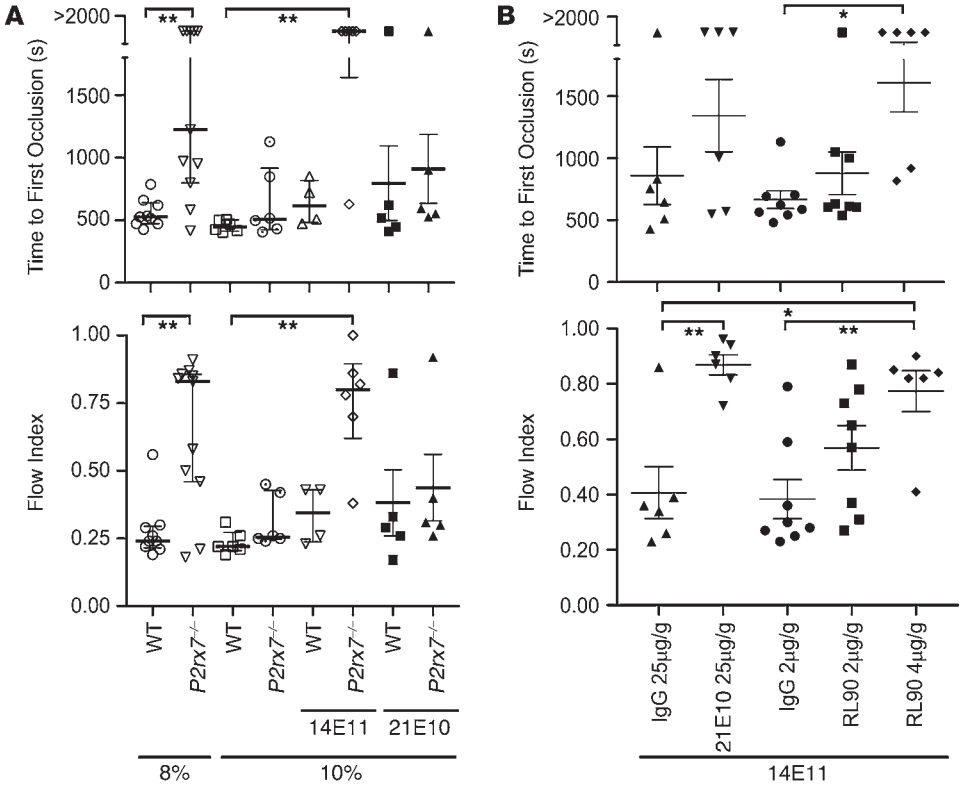

Figure 5

P2rx7$^{-/-}$ mice are protected from thrombosis in the $FeCl_3$-induced carotid artery model. (**A**) Carotid artery injury was induced with 8% or 10% $FeCl_3$•$6H_20$ in C57BL/6 WT and *P2rx7*$^{-/-}$ mice; where indicated, anti-FXI 14E11 (65 ng/g) or anti-TF 21E10 (25 μg/g body weight) were also given prior to injury. (**B**) At 5 minutes before injury with 8% $FeCl_3$•$6H_20$, mice were injected into the contralateral jugular vein with anti-FXI 14E11 (65 ng/g, calculated to inhibit approximately 30% of plasma FXI) with addition of anti-TF 21E10 (25 μg/g body weight), anti-PDI RL90 (2 or 4 μg/g), or corresponding amounts of irrelevant mouse monoclonal IgG. Results for individual mice are shown; horizontal lines and error bars denote median and interquartile range of the time to first occlusion (defined as flow <10% of that measured in the artery before injury) and mean ± SEM of the flow index (ratio between total volume of arterial blood flow after injury and expected volume based on preinjury flow). Flow index of 1 indicates completely unimpeded flow throughout the observation period. Differences in occlusion time were evaluated with the nonparametric Kruskal-Wallis test followed by paired comparisons with the Dunn test; differences in flow index were assessed with 1-way ANOVA followed by Bonferroni test. *$P < 0.05$; **$P < 0.01$.

Hematopoietic and myeloid cells are possible sources for TF$^+$ MPs in thrombus formation (23, 26, 47), but genetic evidence also implicates vessel wall– and SMC-derived TF in arterial thrombosis (1, 2). We therefore generated BM chimeras to address the relative prothrombotic contributions of P2X7 receptor signaling in the vessel wall and hematopoietic compartment. Consistent with previous studies (1, 47), we found no evidence that BM transplantation attenuated thrombus formation under our experimental conditions, but it was important to exclude prothrombotic effects of this procedure. When challenged with 8% $FeCl_3$·$6H_2O$, lethally irradiated *P2rx7*$^{-/-}$ mice receiving *P2rx7*$^{-/-}$ BM cells displayed impaired thrombus formation, and the reduction in flow index (Figure 6A) was similar to that seen with *P2rx7*$^{-/-}$ mice in the absence of BM transplantation, excluding the possibility that lethal irradiation nonspecifically increases thrombogenicity. Vessel wall or hematopoietic cell *P2rx7*$^{-/-}$ mice were generated. Successful engraftment of WT BM into *P2rx7*$^{-/-}$ mice and *P2rx7*$^{-/-}$ BM into WT mice was confirmed by genotyping of blood cell DNA and by ATP-induced TF activation and MP release in BM-derived macrophages isolated from the chimeric mice (Figure 6B). Either kind of BM chimera challenged with 8% or 10% $FeCl_3$·$6H_2O$ after receiving a noninhibitory dose of anti-FXI 14E11 developed vessel occlusion in the time frame normally observed for WT mice, and the carotid arteries remained poorly perfused throughout the observation period (Figure 6A). Thus, reconstitution of P2X7 receptor in either compartment was sufficient to restore vascular occlusion, which indicates that P2X7 receptor functions to promote thrombosis not only in the myeloid and hematopoietic compartment, but also in the vessel wall.

P2X7 receptor regulates TF$^+$ MP release from SMCs. In the vessel wall, the P2X7 receptor is expressed by SMCs, fibroblasts, and endothelial cells (48, 49). In order to address directly the role of SMC P2X7 receptor signaling in TF activation, lung SMCs were isolated that stained uniformly positive for SMA and TF (Figure 7A). Stimulation of SMCs for 30 minutes with 4–5 mM ATP, but not lower concentrations, promoted release of TF$^+$ and integrin β1$^+$ MPs. Western blotting of cell lysates and recovered MPs showed that approximately 10% of the cellular TF and less than 2% of cellular integrin β1 were released in the MP fraction (Figure 7B). SMCs expressed P2X7 receptor protein, which was also detected in *P2rx7*$^{-/-}$ mice (Figure 7C), consistent with the known expression of

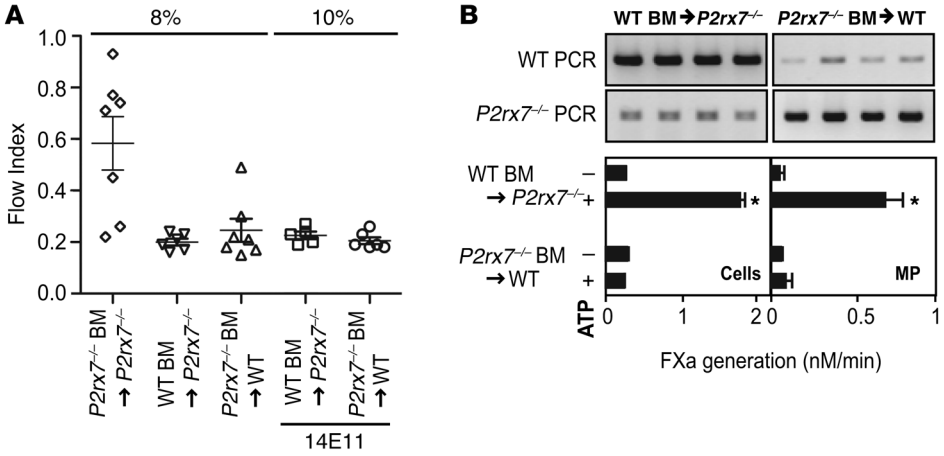

Figure 6

P2X7 receptor signaling in the hematopoietic or vessel wall compartment is sufficient to induce thrombosis. (**A**) Thrombus formation in the carotid artery of control *P2rx7*$^{-/-}$ BM transplants into *P2rx7*$^{-/-}$ mice or BM chimeras with vessel wall or hematopoietic P2X7 receptor deficiency. Mice were challenged with 8% or 10% $FeCl_3$•$6H_2O$ after receiving a noninhibitory dose of anti-FXI 14E11 (65 ng/g). Flow index was determined as in Figure 5. $P < 0.01$, chimera vs. *P2rx7*$^{-/-}$ BM transplant control; ANOVA followed by the Bonferroni test. 2 independent BM transplantation experiments were performed for the chimeric mice. (**B**) Successful engraftment of WT BM into *P2rx7*$^{-/-}$ mice and *P2rx7*$^{-/-}$ BM into WT mice was confirmed by genotyping of blood cell DNA and by ATP-induced TF activation and MP release from BM-derived macrophages isolated from the chimeric mice. Results are from 2 independent experiments performed in triplicate. *$P < 0.01$ vs. control.

the signaling-defective deletion mutant in certain nonmyeloid cell types of these mice (50). *P2rx7*$^{-/-}$ SMCs expressed normal levels of TF and integrin β1, and ATP stimulation of WT, but not *P2rx7*$^{-/-}$, SMCs resulted in the release of MPs that carried TF, integrin β1, actin, and P2X7 receptor, but not PSGL-1 (Figure 7D and data not shown). These MPs were procoagulant (Figure 7E), which established that ATP-induced MP release from SMCs was dependent on P2X7 receptor signaling.

To confirm that ATP induced MP release specifically in the vascular compartment, SMCs were also isolated from adventitia-free aortas. ATP stimulation opens a large solute pore and increases permeability for the cationic dye YO-PRO. Upon ATP stimulation, SMCs from WT mice, but not *P2rx7*$^{-/-}$ mice, showed the expected uptake of YO-PRO (Figure 7F). ATP stimulation of aortic SMCs resulted in 2-fold increased cell surface TF activity and release of procoagulant TF$^+$ MPs carrying integrin β1 (Figure 7G). GFP-expressing SMCs were used in these experiments. GFP was recovered in the MP fraction, which indicates that MPs were generated by an outward budding event that incorporated cytosolic GFP protein. Thus, the prothrombotic effects of both vessel wall and hematopoietic P2X7 receptor signaling can be explained by a common function to promote the release of TF$^+$ MPs.

Rescue of defective P2X7 receptor signaling by an anti-PDI antibody. In testing the effects of anti-PDI monoclonal antibodies on ATP-induced TF activation, we obtained unexpected results with the anti-PDI antibody clone 34 (BD), generated against a fragment consisting mainly of the noncatalytic domain of bovine PDI. This region of PDI contributes to chaperone and nitric oxide binding functions of PDI. A previous study concluded that clone 34 and RL90 behaved similarly to inhibit PDI reductase activity–dependent PS uptake, resulting in increased procoagulant activity of endothelial cells (51). Consistent with this prior demonstration, we found that clone 34 induced PS exposure, as measured by annexin V staining, on WT and *P2rx7*$^{-/-}$ macrophages (Figure 8A). Under the same conditions, RL90 had no similar activity (Figure 2F). As seen with ATP-stimulated cells, reacting free thiols with DTNB did not inhibit PS exposure on clone 34–stimulated cells. The following experiments showed that clone 34 has additional effects consistent with loss of regulatory control or activation of the pathways typically triggered by P2X7 receptor signaling.

P2X7 receptor activation specifically generates a large plasma membrane pore that is permeable to solutes of less than 1,000 Da, such as the cationic dye YO-PRO. The pannexin-1 hemichannel is responsible for rapid opening of the pore after P2X7 receptor activation, but slow dye uptake involves additional pathways (31–34, 52). Whereas RL90 and another anti-PDI monoclonal antibody, SPA-891, produced no change, anti-PDI clone 34 was as effective as ATP at inducing YO-PRO influx in WT macrophages (Figure 8B). This effect was blocked by recombinant N-ethyl maleimide–blocked (NEM-blocked) PDI, demonstrating specificity. Clone 34 also specifically bypassed the defect of *P2rx7*$^{-/-}$ macrophages to restore a functional large solute channel in the absence of ATP stimulation (Figure 8B). Control experiments in P2X7 receptor–deficient HEK 293 cells showed efficient dye flux and TF activation upon stimulation with clone 34, but ATP-induced YO-PRO uptake required P2X7 receptor transfection (Supplemental Figure 6). Thus, clone 34 did not target P2X7 receptor directly. Importantly, blocking free thiols with DTNB severely impaired YO-PRO uptake in ATP- and clone 34–stimulated cells (Figure 8B), providing evidence that this downstream effect of P2X7 receptor activation also involves free thiols.

Clone 34 promoted TF activation and bypassed defective P2X7 receptor signaling to release procoagulant MPs, and preincubation of the antibody with inactive recombinant human PDI abolished these effects (Figure 8C), confirming specificity. In addition, the upregulation of cell and MP activity by clone 34 was inhibited by DTNB, and MPs recovered from clone 34–stimulated cells recapitulated the protein composition of MPs released by ATP stimulation (Figure 8, C and D). Unlike RL90, clone 34 also induced the appearance of free thiols on the cell surface and the release of MPs with proteins carrying solvent-accessible free

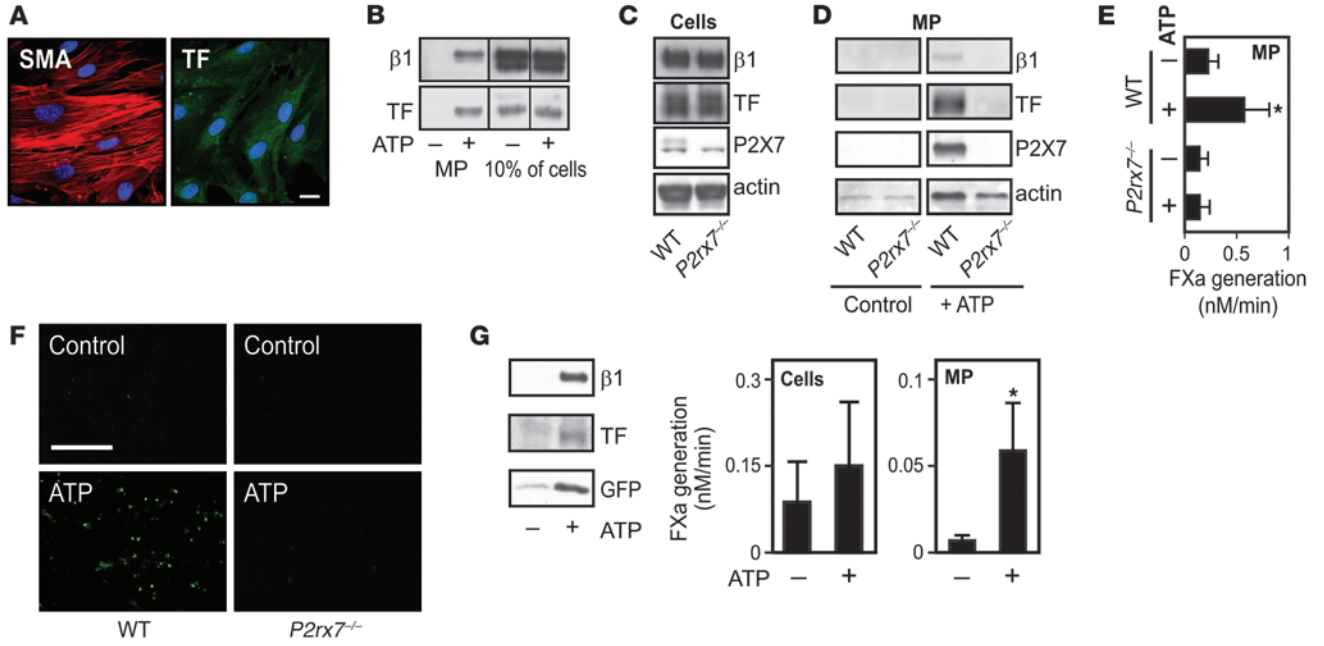

Figure 7

P2X7 receptor signaling regulates TF activation and TF+ MP release from SMCs. (**A**) TF and SMA expression by isolated lung-derived SMCs. Scale bar: 20 μm. (**B**) Western blot of integrin β1 and TF in MPs from ATP-stimulated SMCs relative to the corresponding cell lysates. Lanes for cell lysates were run on the same gel but were noncontiguous. (**C**) P2X7 receptor expression by WT and *P2rx7*$^{-/-}$ lung SMCs, determined by Western blotting. A slower migrating, possibly glycosylation or splice isoform of the P2X7 receptor was absent from cells of *P2rx7*$^{-/-}$ mice. No difference in expression of integrin β1, TF, and actin was observed between WT and *P2rx7*$^{-/-}$ cells. (**D** and **E**) Protein composition and TF activity of MPs released from ATP-stimulated WT and *P2rx7*$^{-/-}$ lung-derived SMCs. P2X7 receptor in WT MPs had a mobility corresponding to the slower migrating isoform in **C**. (**F**) P2X7 receptor stimulation induced aortic SMC uptake of YO-PRO (10 μM), added during ATP stimulation. Scale bar: 250 μm. (**G**) TF protein content and TF-dependent FXa generation in MPs from ATP-stimulated aortic WT SMCs ($n \geq 3$). SMCs were isolated from transgenic mice expressing GFP ubiquitously in all cells in order to monitor MP release based on packaging of cytosolic content. *$P < 0.05$ vs. control.

thiols from WT and *P2rx7*$^{-/-}$ macrophages (Figure 8E and data not shown). The only difference in the pattern of labeled MP proteins was the persistent labeling of the 54-kDa band in clone 34–treated cells, as labeling of this protein disappeared in WT or *P2rx7*$^{-/-}$ macrophages in the course of stimulation with ATP. Although this protein has thus far eluded attempts for identification, it appeared that the regulatory functions of PDI in the MP release pathway involved both reductive and oxidative changes. Clone 34 also induced the release of procoagulant MPs from aortic SMCs (Figure 8F), confirming that the activating effect of this antibody was not restricted to myeloid cells.

Anti-PDI clone 34 restores TF-dependent thrombosis in P2rx7$^{-/-}$ *mice.* The bypassing of defective TF decryption and TF+ MP release of *P2rx7*$^{-/-}$ cells by clone 34 predicted a prothrombotic effect of this antibody in thrombosis-resistant *P2rx7*$^{-/-}$ mice. Indeed, all *P2rx7*$^{-/-}$ mice treated with clone 34 developed a stable occluding thrombus, whereas *P2rx7*$^{-/-}$ mice showed reduced carotid artery thrombosis after the same 8% $FeCl_3 \cdot 6H_2O$ injury (Figure 9). Injecting a noninhibitory dose of anti-FXI 14E11 caused a small, but not significant, impairment of thrombus formation and stability in *P2rx7*$^{-/-}$ mice treated with clone 34, but concomitant administration of anti-TF 21E10 with the same dose of anti-FXI 14E11 prevented stable occlusion in all treated mice. These data support the conclusion that direct activation of PDI bypasses the signaling defect of *P2rx7*$^{-/-}$ mice to induce the TF pathway in thrombosis.

Discussion

The present data connect activation of the P2X7 receptor complex to a PDI-regulated thiol pathway that controls the stimulated release of procoagulant TF+ MPs and TF-dependent thrombosis. Although PS plays an essential role in TF-initiated coagulation reactions, it can be difficult to distinguish between TF activation and the increased availability of procoagulant PS in cellular models of incompletely encrypted TF (5, 6, 51). The current experiments were performed in macrophages with largely encrypted TF and provided evidence that TF activation and release on MPs cannot be explained by increased extracellular availability of PS alone, but rather involves thiol exchange and PDI function. PDI is positioned in the P2X7 receptor TF activation pathway, since blocking PDI with the antithrombotic antibody RL90 prevented the release of procoagulant MPs, whereas an alternative antibody to PDI produced opposing effects that mimicked cellular activation by P2X7 receptor signaling in several aspects. It was proposed that PDI released from injured cells activates TF on circulating MPs (21). The demonstrated inhibition of MP release by RL90 suggests an alternative role for cell surface PDI to act as a critical regulatory component in the P2X7 receptor pathway that generates TF+ MPs in thrombosis.

Activation of the P2X7 receptor results in reductive changes of the cell surface and MPs. Although the antithrombotic RL90 and the activating clone 34 both inhibit PDI reductase activity (51), these antibodies produced opposite effects upon solvent-accessible

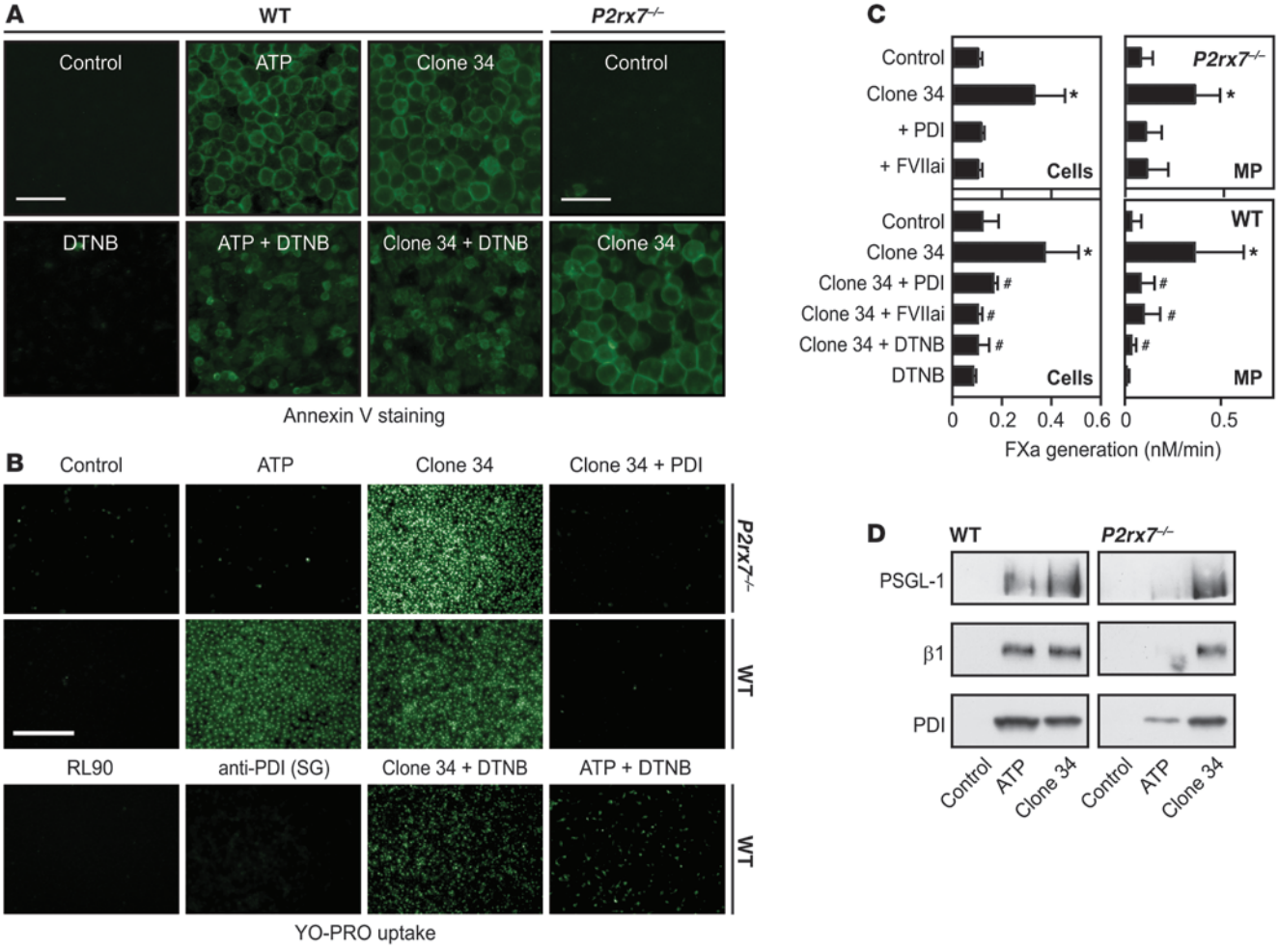

Figure 8

Anti-PDI bypasses defective P2X7 receptor signaling to activate TF and MP release. (**A**) PS exposure on WT and *P2rx7*$^{-/-}$ macrophages stimulated with ATP (5 mM) or anti-PDI clone 34 (10 μg/ml) for 30 minutes. Extracellular free thiols were blocked with DTNB (2 mM) as indicated. Images are representative of 3 independent experiments. Scale bars: 500 μm. (**B**) Anti-PDI clone 34 induced YO-PRO uptake in WT macrophages similar to ATP stimulation and bypassed the *P2rx7*$^{-/-}$ macrophage signaling defect. RL90 and SPA-891 (SG) did not. NEM-blocked PDI demonstrated antibody specificity. DTNB reduced YO-PRO uptake. Time course experiments further excluded effects on YO-PRO uptake by RL90 at earlier times (not shown). Shown is a typical experiment of 4. Scale bars: 250 μm. (**C**) Anti-PDI clone 34 bypassed the *P2rx7*$^{-/-}$ macrophage signaling defect to induce TF cellular activity and procoagulant MP release. Specificity controls included NEM-blocked PDI (80 μg/ml) and FVIIai (100 nM). DTNB significantly diminished clone 34–induced TF activation and MP activity ($n \geq 4$). $^{*}P < 0.01$ vs. control; $^{\#}P < 0.02$ vs. clone 34 alone. (**D**) Protein composition of MPs released by ATP or by clone 34. Blots are representative of 3 independent experiments. (**E**) Labeling of free thiols with MPB (100 μM) indicated reductive changes on clone 34–released MP. Arrowhead denotes the 54-kDa band differentiating clone 34 from ATP stimulation. (**F**) Anti-PDI clone 34 stimulated release of procoagulant MPs from aortic SMCs ($n \geq 3$). $^{*}P < 0.05$ vs. control.

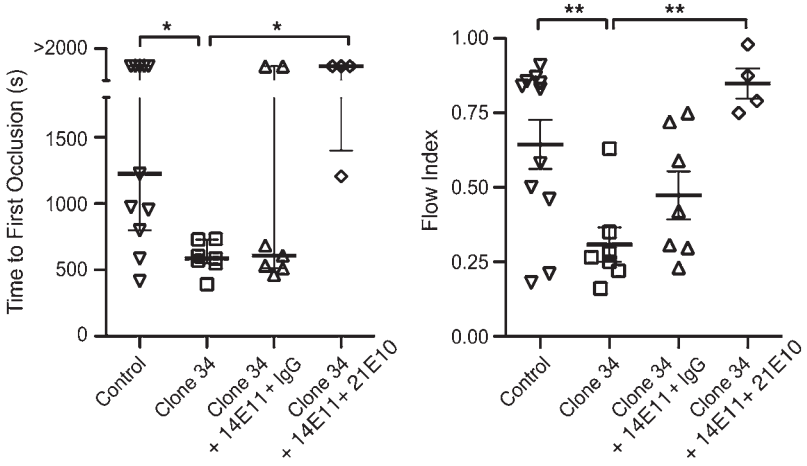

Figure 9
Bypassing activity of anti-PDI clone 34 in *P2rx7*$^{-/-}$ mice to induce TF-dependent thrombosis. Clone 34 (50 μg/mouse) restored vascular occlusion in *P2rx7*$^{-/-}$ mice subjected to 8% $FeCl_3$•$6H_2O$ carotid artery injury. The noninhibitory dose of anti-FXI 14E11 (65 ng/g) did not significantly reverse the effect of clone 34 injection. Combined treatment with anti-TF 21E10 (25 μg/g body weight) and anti-FXI 14E11 prevented the thrombosis-promoting effect of clone 34 in *P2rx7*$^{-/-}$ mice. Results are presented and differences evaluated as in Figure 5; controls are reproduced from Figure 5A for comparison. *$P < 0.05$; **$P < 0.01$.

thiol exposure, and only RL90 attenuated MP release. RL90 also inhibits PDI denitrosylase activity (42), but we could not conclusively establish whether clone 34 activates PDI denitrosylase activity or influences functions of the hydrophobic pocket of PDI that include nitric oxide sequestration (18, 19). PDI regulates NADPH oxidase (53), and P2X7 receptor signaling triggers NADPH oxidase–dependent protein denitrosylation (41). Our data showed that blocking NADPH oxidase with the flavoenzyme inhibitor DPI or preventing ROS production with NAC attenuated the release of TF^+ procoagulant MPs. Taken together with the inhibitory effects of thiol blockade with DTNB, these data demonstrate an essential role for thiol exchange reactions and ROS in the P2X7 receptor signaling pathways leading to the activation of prothrombotic TF.

Recent data showed that endothelial cell activation by a laser pulse induces the release of PDI from endothelial cells, leading to rapid accumulation of PDI at sites of injury and fibrin formation that is significantly inhibited by RL90 (54, 55). Whereas this nonocclusive, mild arteriolar injury is dependent on TF synthesized by the hematopoietic, myeloid compartment (47, 56), occlusive $FeCl_3$ injury of the carotid artery is more complex. It also depends on TF derived from SMCs (2), as well as substantial contributions from intrinsic coagulation activation (44, 45). However, pharmacologic blockade of PDI with RL90 or of TF with an inhibitory antibody were similarly effective to prevent stable vessel occlusion, demonstrating contributions of TF and PDI to thrombosis in $FeCl_3$ injury. Genetic inactivation of P2X7 signaling had a pronounced antithrombotic effect in this model, and the presented antibody inhibition experiments in a more severe $FeCl_3$ challenge provided evidence that P2X7 receptor deficiency impairs TF-dependent thrombosis.

The previous finding that ATP stimulation of the P2X7 receptor releases TF^+ MPs from monocyte-derived dendritic cells (28) was shown here to have broad implications for TF activation in thrombosis. The P2X7 receptor induces MP release not only from myeloid cells, but also SMCs, which indicates that local MP generation in the vessel wall may contribute to thrombus growth. Consistently, P2X7 receptor in the vessel wall or the hematopoietic compartment can drive thrombus formation and reverse the protection of *P2rx7*$^{-/-}$ mice from vascular occlusions in the high-flow model of $FeCl_3$-induced arterial thrombosis. Although genetic deletion of TF in SMCs indicated that prothrombotic TF is mainly localized in the vessel wall TF in the $FeCl_3$ model (2), our data suggest that TF^+ MPs generated by the P2X7 receptor pathway in either hematopoietic or vessel wall cells complement cellular sources of SMC-expressed TF. These data challenge the simplistic view that loss of vascular integrity is sufficient to trigger TF-dependent thrombosis and provide what we believe to be the first identification of a cell signaling pathway contributing to the activation of prothrombotic TF in vivo.

Additional components of the P2X7 receptor signaling complex may also be connected, directly or indirectly, to the prothrombotic response. P2X7 receptor is associated with integrins (35), known targets for regulation by PDI (57, 58). PDI regulates NADPH oxidase (53), and the rapid change of the redox environment after P2X7 receptor stimulation (41) may influence the endothelium, blood cells, or platelets. Because ATP is rapidly released from injured cells, P2X7 receptor signaling may play a major role in precipitating acute thrombotic events in atherosclerosis, where TF is expressed in inflammatory and vessel wall cells (59, 60). P2X7 receptor is crucial for the release of IL-1β (30), linking TF activation to a major proinflammatory pathway with intriguing implications for the close link of thrombosis and inflammation in cardiovascular disease. Because *P2rx7*$^{-/-}$ mice did not exhibit substantial hemostatic impairment, targeting P2X7 receptor may represent an unconventional approach to anticoagulant therapy that disables prothrombotic TF activation, instead of neutralizing coagulation proteases, while disarming unregulated local inflammatory reactions.

Methods

Mice and isolation of primary cells. All animal procedures with *P2rx7*$^{-/-}$ mice, carrying signaling-defective P2X7 receptor as a result of a partial deletion in the cytoplasmic domain (43), and WT C57BL/6 controls (Jackson) were approved by the IACUC of the Scripps Research Institute. BM chimeras were generated by injecting mice intravenously with 5–10 × 10^6 BM cells after 4–6 hours of lethal irradiation. Mice were analyzed in the thrombosis model no earlier than 8 weeks after engraftment and after confirmation of blood genotypes by semiquantitative PCR.

BM-derived macrophages were generated as previously described (36) and used on day 7 for experiments. Lung SMCs were expanded from mouse lung endothelial cell preparations by propagation in medium lacking endothelial growth factors. Briefly, after collagenase digestion of lungs, cells were cultured in flasks coated with 0.2% gelatin (Sigma-Aldrich) in RPMI medium containing 20% heat-inactivated FCS, nonessential amino acids, 2-mercaptoethanol (Invitrogen), and antibiotics. SMCs derived from murine aortas cleaned of surrounding fat tissues and the adventitia layer were isolated using published protocols (61) and

cultured on gelatin-coated flasks in DMEM containing 20% FCS and 50 μg/ml ascorbic acid (Wako Chemicals). For some experiments, SMCs were isolated from mice carrying a transgene for GFP under the control of the chicken actin promoter (C57BL/6-Tg[CAG-EGFP]131Osb/LeySopJ; Jackson).

MP release assay, TF procoagulant activity, and prothrombinase assay. Macrophages (1×10^6 cells/well) were seeded in 12-well plates. In all experiments reported, macrophages were first primed overnight with 100 ng/ml interferon-γ (Peprotech), followed by addition of 1 μg/ml LPS (Enzo Life Sciences) for 4 hours before MP release. After a brief wash, cells were stimulated in a saline solution (130 mM Na gluconate, 5 mM glucose, 5 mM glycine, 20 mM Hepes, 5 mM KCl, 1 mM $MgCl_2$) (62) with 5 mM ATP (Roche) or 10 μM ionomycin (EMD Chemicals) for 30 minutes, unless otherwise indicated. In control experiments, 2 mM $CaCl_2$ was added to the release buffer.

Thiols were blocked by a brief pretreatment (~2 minutes) with 1 mM NEM (Sigma-Aldrich) or 2 mM DTNB (EMD Chemicals) in the saline solution before stimulation with ATP or ionomycin. The NADPH oxidase inhibitor DPI (100 μM) was added for 30–120 minutes prior to and during ATP stimulation. The ROS inhibitor NAC (3 mM) buffered with HEPES to pH 7.4 was added for 120 minutes prior to and during ATP stimulation.

Anti-PDI clone 34 (10 μg/ml; BD Biosciences) was added to the release buffer for the same duration as used for ATP stimulation, typically 30 minutes. As control, 80 μg/ml of NEM-blocked recombinant PDI was preincubated for 15 minutes with the antibody prior to addition to the cells. RL90 (10–20 μg/ml; Thermo Fisher Scientific) or mouse monoclonal SPA-891 (Stressgene) were preincubated for 15 minutes with macrophages before stimulation with ATP. To assure stability, antibodies were kept in the manufacturer's buffers. Potential artifacts as a result of buffer composition were excluded in control experiments in vitro that used antibodies that were buffer exchanged to 20 mM Hepes, 150 mM NaCl, pH 7.4. All experiments in mice in vivo used stock solutions of antibodies at 1 mg/ml exchanged to the Hepes buffer.

Release of MPs from macrophages was evaluated by FACS or by fluorescent labeling of membrane lipids. For FACS analysis, cell-free supernatant MP counts were quantified on a LSR-II flow cytometer (BD) using defined platelet suspensions to define submicron gates and to calibrate the event counts between individual experiments. Lipids were labeled with NBD (Invitrogen) (39). Cells were stimulated with ATP or ionomycin in the presence of 3 μM NBD for 30 minutes, and MPs were recovered from cell-free supernatants. MP contents were quantified by measuring fluorescence at 536 nm of the lipophilic dye after excitation with 466 nm.

Lung and aortic SMCs were seeded in 12-well plates in DMEM 1–2 days before the MP release assay that was carried out in serum-free DMEM with stimuli as described above. After stimulation of SMCs or macrophages, cell-free supernatants were prepared by centrifugation for 10 minutes at 800 *g*, and MPs were recovered by centrifugation of the supernatant at 16,000 *g* for 1 hour.

TF procoagulant activity was determined by 2-stage chromogenic assay using mouse FVIIa (provided by L. Petersen, Novo Nordisk, Malov, Denmark) and human plasma–derived factor X (FX; 36). For this assay, cells were first washed in 10 mM Hepes, 150 mM NaCl, 5.3 mM KCl, 1.5 mM Ca^{2+}, pH 7.4, followed by incubation at 37°C with FVIIa/FX for defined times. Similarly, the collected MPs after centrifugation were resuspended in HBS buffer containing FVIIa/FX. For surface biotinylation, macrophages were incubated for 15 minutes at room temperature with 2 mM NHS-Biotin (Thermo Fisher Scientific) either before or after stimulation with ATP. The reagent was quenched by washing cells with Tris buffer, followed by FXa generation assay with or without cell lysis using 15 mM octylglucoside.

Prothrombinase activity on stimulated macrophages was determined by incubation with 10 nM FVa, 5 nM FXa, and 0.5 μM prothrombin (Haematologic Technologies) in HBS buffer. After defined times, the reactions were quenched in EDTA buffer, and thrombin levels were assessed with the chromogenic substrate Spectrozyme TH (American Diagnostica).

Western blotting and labeling of free thiols. Western blotting was used to detect antigen expression levels in cells, and MPs were collected by centrifugation. Because of low protein yield of recovered MPs, samples were typically pooled from several wells for Western blotting. Antibodies for Western blotting were as follows: TF polyclonal or monoclonal 11F6, generated in our laboratory to recombinant mouse TF extracellular domain; PSGL-1 (monoclonal rat anti-mouse CD162; BD Biosciences); polyclonal anti–integrin β1 (provided by M.H. Ginsberg, UCSD, La Jolla, California, USA); PDI (clone 34, BD Biosciences); and actin, GFP, and P2X7 receptor (Sigma-Aldrich).

Free thiols on cells and MPs were labeled with 100 μM MPB (Cayman Chemical) in the release buffer during the 30-minute stimulation or by incubating cell free-MP supernatant for 10 minutes at 4°C after the release reaction. Labeling reactions were quenched with 2 mM cysteine (Sigma-Aldrich). After electrophoretic transfer, membranes were probed for biotinylated proteins with streptavidin-HRP conjugate (Thermo Fisher Scientific) and quantification by densitometry using NIH ImageJ software.

Tail bleeding times. In the tail clipping assay (63), mice were anesthetized, and the distal portion of the tail with a diameter of 2 mm was cut and immersed in 37°C saline until spontaneous cessation of bleeding occurred. Blood loss was quantified by measuring the hemoglobin content of collected erythrocytes lysed with red blood lysis solution (Sigma-Aldrich) for 3 minutes. Hemoglobin content of lysates in 6 ml saline was determined by measuring absorbance at 575 nm.

Carotid artery $FeCl_3$-induced thrombosis model. Blood flow was measured by a miniature ultrasound flow probe positioned around the isolated left common carotid artery, and $FeCl_3$ injury was induced by a carefully dispensed 0.7-μl drop of 8% (0.30 M Fe^{3+}) or 10% (0.37 M Fe^{3+}) freshly prepared $FeCl_3 \cdot 6\ H_2O$ placed on the exposed adventitia for 3 minutes. After wash with warm physiologic saline, carotid blood flow monitoring was continued for 30 minutes. Time to first occlusion after initiation of injury was the time required for a decrease of blood flow to less than 10% of the value initially measured in the uninjured artery. The flow index was calculated as the ratio of the total volume of blood that flowed through the artery after injury (integration of flow measured in ml/min and sampled every second) and the expected flow in the 30-minute observation period (flow measured before injury multiplied by 30). Antibodies were injected through a catheter placed in the right jugular vein at the following doses: anti-FXI 14E11, 65 ng/g body weight (45); anti-TF 21E10, 25 μg/g; anti-PDI clone 34, 50 μg/mouse; anti-PDI RL90, 2 or 4 μg/g body weight. All antibodies were exchanged to buffers prepared with pyrogen-free water.

Ex vivo perfusion experiments. Macrophages adherent to glass coverslips were stimulated for 15–30 minutes with 5 mM ATP in 20 mM Hepes, pH 7.4, buffered growth medium. Coverslips were then rinsed and assembled at the bottom of a rectangular flow chamber with a 125-μm height maintained by a silicon gasket. Blood was drawn from the inferior vena cava of anesthetized WT mice into a syringe containing citrate-phosphate-dextrose (11 mM sodium citrate, 14 mM dextrose, 1.7 mM citric acid, and 1.6 mM monobasic sodium phosphate). Blood was recalcified with 5 mM $CaCl_2$, and an optimized concentration of Lepirudin (450 nM; recombinant [Leu1-Thr2]-63-desulfohirudin; Refludan; Bayer Corp.) was added to prevent clotting inside the flow apparatus before reaching the cell surface. Cell and platelet visualization was achieved by adding quinacrine-HCl (mepacrine; 10 μg/ml; Sigma-Aldrich) to the perfused blood. Deposited fibrin was visualized with Alexa Fluor

546–labeled (Invitrogen) mouse monoclonal IgG (50 μg/ml) specific for the B chain of mouse and human fibrin after removal of fibrinopeptide B (HB-8545; ATCC). Blood (200 μl) was perfused with a syringe pump (Harvard Apparatus Inc.) at a flow rate of 0.162 ml/min, corresponding to a wall shear rate of 500 s^{-1}, followed by buffer (DMEM) for 2 minutes to facilitate fibrin quantification by confocal *z* section analysis using a Zeiss Axiovert 135M/LSM 410 microscope (Carl Zeiss) and Plan-Apochromat ×63/1.40 NA oil immersion objective. Image analysis was performed with NIH ImageJ64: deposited fibrin volume was measured from confocal sections (*z* interval, 1 or 2 μm) collected at 4 different positions in the flow chamber (2.5, 5, 10, and 20 mm distance from inlet along the centerline of the flow path). Total fibrin-covered area per section was calculated as the sum of all values multiplied by the *z* interval.

Fluorescence microscopy. ATP-dependent increase in membrane permeability for high–molecular weight solutes was determined by measuring the uptake of 10 μM of the fluorescent dye YO-PRO (Invitrogen) (64) in cells stimulated with 5 mM ATP for 30 minutes. In control experiments, HEK-293 cells (ATCC) were transfected with 1 μg hP2X7-EE tagged plasmid (gift of P. Pelegrin and A. Surprenant; University of Manchester, Manchester, United Kingdom) using Lipofectamine 2000 reagent (Invitrogen). Cells were used 24 hours after transfection for YO-PRO uptake experiments. PS exposure was detected by poststimulation staining with annexin V FITC conjugate (BD Biosciences) according to the manufacturer's protocol. Images were taken with ×10–×40 Nikon objectives on a Nikon Eclipse Fluorescent microscope. Permeabilized SMCs were stained with PE-labeled anti-SMA (Sigma-Aldrich), and nonpermeabilized SMCs were stained with FITC-coupled rat anti-mouse TF 11F6.

Statistics. Unless otherwise indicated, statistical analysis was by 2-tailed Student's *t* test, and data are shown as mean ± SD. A *P* value less than 0.05 was considered significant.

Acknowledgments

This study was supported by NIH grant HL-31950 (to W. Ruf and Z.M. Ruggeri) and an American Heart Association California Affiliate Fellowship (to C. Furlan-Freguia). We thank Jennifer Royce, Cindi Biazak, and Pablito Tejada for technical support; Antonella Zampolli for help with intravital mouse studies; Florence Schaffner for assistance in immune histochemistry; and Cheryl Johnson for the preparation of figures.

Received for publication April 6, 2011, and accepted April 27, 2011.

Address correspondence to: Wolfram Ruf, Department of Immunology and Microbial Science, Scripps Research Institute, 10550 North Torrey Pines Road, La Jolla, California 92037, USA. Phone: 858.784.2748; Fax: 858.784.8480; E-mail: ruf@scripps.edu.

1. Day SM, et al. Macrovascular thrombosis is driven by tissue factor derived primarily from the blood vessel wall. *Blood*. 2005;105(1):192–198.
2. Wang L, Miller C, Swarthout RF, Rao M, Mackman N, Taubman MB. Vascular smooth muscle-derived tissue factor is critical for arterial thrombosis after ferric chloride-induced injury. *Blood*. 2009; 113(3):705–713.
3. Bach RR. Tissue factor encryption. *Arterioscler Thromb Vasc Biol*. 2006;26(3):456–461.
4. Kothari H, Rao LVM, Pendurthi U. Cys186-Cys209 disulfide-mutated tissue factor does not equal cryptic tissue factor: no impairment in decryption of disulfide mutated tissue factor. *Blood*. 2010;116:502–503.
5. Kothari H, Nayak RC, Rao LV, Pendurthi UR. Cystine186-cystine 209 disulfide bond is not essential for the procoagulant activity of tissue factor or for its de-encryption. *Blood*. 2010;115(21):4273–4283.
6. Pendurthi UR, Ghosh S, Mandal SK, Rao LV. Tissue factor activation: is disulfide bond switching a regulatory mechanism? *Blood*. 2007;110(12):3900–3908.
7. Ahamed J, et al. Disulfide isomerization switches tissue factor from coagulation to cell signaling. *Proc Natl Acad Sci U S A*. 2006;103(38):13932–13937.
8. Chen VM, Ahamed J, Versteeg HH, Berndt MC, Ruf W, Hogg PJ. Evidence for activation of tissue factor by an allosteric disulfide bond. *Biochemistry*. 2006;45(39):12020–12028.
9. Liang HP, Hogg PJ. Critical importance of the cell system when studying tissue factor de-encryption. *Blood*. 2008;112(3):912–913.
10. Ruf W, Versteeg HH. Tissue factor mutated at the allosteric Cys186-Cys209 disulfide bond is severely impaired in decrypted procoagulant activity. *Blood*. 2010;116(3):500–501.
11. Krudysz-Amblo J, Jennings ME, Mann KG, Butenas S. Carbohydrates and activity of natural and recombinant tissue factor. *J Biol Chem*. 2010; 285(5):3371–3382.
12. Sevinsky JR, Rao LVM, Ruf W. Ligand-induced protease receptor translocation into caveolae: A mechanism for regulating cell surface proteolysis of the tissue factor-dependent coagulation pathway. *J Cell Biol*. 1996;133(2):293–304.
13. Mandal SK, Iakhiaev A, Pendurthi UR, Rao LV. Acute cholesterol depletion impairs functional expression of tissue factor in fibroblasts: modulation of tissue factor activity by membrane cholesterol. *Blood*. 2005;105(1):153–160.
14. Dietzen DJ, Page KL, Tetzloff TA. Lipid rafts are necessary for tonic inhibition of cellular tissue factor procoagulant activity. *Blood*. 2004;103(8):3038–3044.
15. Bhattacharjee G, et al. Regulation of Tissue Factor-Mediated Initiation of the Coagulation Cascade by Cell Surface Grp78. *Arterioscler Thromb Vasc Biol*. 2005;25(8):1737–1743.
16. Bach RR, Moldow CF. Mechanism of tissue factor activation on HL-60 cells. *Blood*. 1997;89(9):3270–3276.
17. Le D, Rapaport S, Rao LVM. Studies of the mechanism for enhanced cell surface factor VIIa\tissue factor activation of factor X on fibroblast monolayers after their exposure to N-ethylmaleimide. *Thromb Haemost*. 1994;72(6):848–855.
18. Ramachandran N, Root P, Jiang XM, Hogg PJ, Mutus B. Mechanism of transfer of NO from extracellular S-nitrosothiols into the cytosol by cell-surface protein disulfide isomerase. *Proc Natl Acad Sci U S A*. 2001;98(17):9539–9544.
19. Sliskovic I, Raturi A, Mutus B. Characterization of the S-denitrosation activity of protein disulfide isomerase. *J Biol Chem*. 2005;280(10):8733–8741.
20. Versteeg HH, Ruf W. Tissue factor coagulant function is enhanced by protein-disulfide isomerase independent of oxidoreductase activity. *J Biol Chem*. 2007;282(35):25416–25424.
21. Reinhardt C, et al Protein disulfide isomerase acts as an injury response signal that enhances fibrin generation via tissue factor activation. *J Clin Invest*. 2008;118(3):1110–1122.
22. Cho J, Furie BC, Coughlin SR, Furie B. A critical role for extracellular protein disulfide isomerase during thrombus formation in mice. *J Clin Invest*. 2008;118(3):1123–1131.
23. Falati S, et al. Accumulation of tissue factor into developing thrombi in vivo is dependent upon microparticle P-selectin glycoprotein ligand 1 and platelet P-selectin. *J Exp Med*. 2003;197(11):1585–1598.
24. Falati S, Gross P, Merrill-Skoloff G, Furie BC, Furie B. Real-time in vivo imaging of platelets, tissue factor and fibrin during arterial thrombus formation in the mouse. *Nat Med*. 2002;8(10):1175–1181.
25. Furie B, Furie BC. Mechanisms of thrombus formation. *N Engl J Med*. 2008;359(9):938–949.
26. Hrachovinova I, et al. Interaction of P-selectin and PSGL-1 generates microparticles that correct hemostasis in a mouse model of hemophilia A. *Nat Med*. 2003;9(8):1020–1025.
27. Del Conde I, Shrimpton CN, Thiagarajan P, Lopez JA. Tissue-factor-bearing microvesicles arise from lipid rafts and fuse with activated platelets to initiate coagulation. *Blood*. 2005;106(5):1604–1611.
28. Baroni M, et al. Stimulation of P2 (P2X7) receptors in human dendritic cells induces the release of tissue factor-bearing microparticles. *FASEB J*. 2007;21(8):1926–1933.
29. Di Virgilio F, et al. Cytolytic P2X purinoceptors. *Cell Death Differ*. 1998;5(3):191–199.
30. DiVirgilio F. Liaisons dangereuses: P2X(7) and the inflammasome. *Trends Pharmacol Sci*. 2007; 28(9):465–472.
31. Pelegrin P, Surprenant A. Pannexin-1 mediates large pore formation and interleukin-1beta release by the ATP-gated P2X7 receptor. *EMBO J*. 2006; 25(21):5071–5082.
32. Pelegrin P, Surprenant A. The P2X(7) receptor-pannexin connection to dye uptake and IL-1beta release. *Purinergic Signal*. 2009;5(2):129–137.
33. Pelegrin P, Surprenant A. Pannexin-1 couples to maitotoxin- and nigericin-induced interleukin-1beta release through a dye uptake-independent pathway. *J Biol Chem*. 2007;282(4):2386–2394.
34. Cankurtaran-Sayar S, Sayar K, Ugur M. P2X7 receptor activates multiple selective dye-permeation pathways in RAW 264.7 and human embryonic kidney 293 cells. *Mol Pharmacol*. 2009;76(6):1323–1332.
35. Kim M, Jiang LH, Wilson HL, North RA, Surprenant A. Proteomic and functional evidence for a P2X7 receptor signalling complex. *EMBO J*. 2001;20(22):6347–6358.
36. Ahamed J, et al. Regulation of macrophage procoagulant responses by the tissue factor cytoplasmic domain in endotoxemia. *Blood*. 2007; 109(12):5251–5259.
37. Aga M, et al. Modulation of monocyte signaling and pore formation in response to agonists of the nucleotide receptor P2X(7). *J Leukoc Biol*. 2002;72(1):222–232.
38. Roy S, Hass PE, Bourell JH, Henzel WJ, Vehar GA. Lysine residues 165 and 166 are essential for the cofactor function of tissue factor. *J Biol Chem*. 1991;266(32):22063–22066.

39. Bianco F, et al. Acid sphingomyelinase activity triggers microparticle release from glial cells. *EMBO J*. 2009;28(8):1043–1054.
40. Moore SF, MacKenzie AB. Murine macrophage P2X7 receptors support rapid prothrombotic responses. *Cell Signal*. 2007;19(4):855–866.
41. Hewinson J, Moore SF, Glover C, Watts AG, MacKenzie AB. A key role for redox signaling in rapid P2X7 receptor-induced IL-1 beta processing in human monocytes. *J Immunol*. 2008;180(12):8410–8420.
42. Root P, Sliskovic I, Mutus B. Platelet cell-surface protein disulphide-isomerase mediated S-nitrosoglutathione consumption. *Biochem J*. 2004; 382(pt 2):575–580.
43. Solle M, et al. Altered cytokine production in mice lacking P2X(7) receptors. *J Biol Chem*. 2001; 276(1):125–132.
44. Renne T, et al. Defective thrombus formation in mice lacking coagulation factor XII. *J Exp Med*. 2005;202(2):271–281.
45. Cheng Q, et al. A role for factor XIIa-mediated factor XI activation in thrombus formation in vivo. *Blood*. 2010;116(19):3981–3989.
46. Ruf W, Edgington TS. An anti-tissue factor monoclonal antibody which inhibits TF:VIIa complex is a potent anticoagulant in plasma. *Thromb Haemost*. 1991;66(5):529–533.
47. Chou J, Mackman N, Merrill-Skoloff G, Pedersen B, Furie BC, Furie B. Hematopoietic cell-derived microparticle tissue factor contributes to fibrin formation during thrombus propagation. *Blood*. 2004;104(10):3190–3197.
48. Cario-Toumaniantz C, Loirand G, Ladoux A, Pacaud P. P2X7 receptor activation-induced contraction and lysis in human saphenous vein smooth muscle. *Circ Res*. 1998;83(2):196–203.
49. Skaper SD, Debetto P, Giusti P. P2X7 receptors in neurological and cardiovascular disorders. *Cardiovasc Psychiatry Neurol*. 2009;2009:861324.
50. Sim JA, Young MT, Sung HY, North RA, Surprenant A. Reanalysis of P2X7 receptor expression in rodent brain. *J Neurosci*. 2004;24(28):6307–6314.
51. Popescu NI, Lupu C, Lupu F. Extracellular protein disulfide isomerase regulates coagulation on endothelial cells through modulation of phosphatidylserine exposure. *Blood*. 2010;116(6):993–1001.
52. Zhang L, Deng T, Sun Y, Liu K, Yang Y, Zheng X. Role for nitric oxide in permeability of hippocampal neuronal hemichannels during oxygen glucose deprivation. *J Neurosci Res*. 2008;86(10):2281–2291.
53. Janiszewski M, et al. Regulation of NAD(P)H oxidase by associated protein disulfide isomerase in vascular smooth muscle cells. *J Biol Chem*. 2005;280(49):40813–40819.
54. Atkinson BT, Jasuja R, Chen V, Nandivada P, Furie B, Furie BC. Laser-induced endothelial cell activation supports fibrin formation. *Blood*. 2010; 116(22):4675–4683.
55. Jasuja R, Furie B, Furie BC. Endothelium-derived but not platelet-derived protein disulfide isomerase is required for thrombus formation in vivo. *Blood*. 2010;116(22):4665–4674.
56. Chen V, et al. Intravascular but not extravascular tissue factor is required for fibrin generation during thrombus formation in cremaster arterioles in living mice subjected to laser injury. *Blood*. 2009;114:140–141.
57. Lahav J, et al. Enzymatically catalyzed disulfide exchange is required for platelet adhesion to collagen via integrin $\alpha_2\beta_1$. *Blood*. 2003;102(6):2085–2092.
58. Swiatkowska M, Szymanski J, Padula G, Cierniewski CS. Interaction and functional association of protein disulfide isomerase with alphaVbeta3 integrin on endothelial cells. *FEBS J*. 2008;275(8):1813–1823.
59. Mach F, Schönbeck U, Bonnefoy JY, Pober JS, Libby P. Activation of monocyte/macrophage functions related to acute atheroma complication by ligation of CD40 - Induction of collagenase, stromelysin, and tissue factor. *Circulation*. 1997;96(2):396–399.
60. Schönbeck U, et al. CD40 ligation induces tissue factor expression in human vascular smooth muscle cells. *Am J Pathol*. 2000;156(1):7–14.
61. Fogelstrand P, Feral CC, Zargham R, Ginsberg MH. Dependence of proliferative vascular smooth muscle cells on CD98hc (4F2hc, SLC3A2). *J Exp Med*. 2009;206(11):2397–2406.
62. Qu Y, Franchi L, Nunez G, Dubyak GR. Nonclassical IL-1 beta secretion stimulated by P2X7 receptors is dependent on inflammasome activation and correlated with exosome release in murine macrophages. *J Immunol*. 2007;179(3):1913–1925.
63. Schlachterman A, et al. Factor V Leiden improves in vivo hemostasis in murine hemophilia models. *J Thromb Haemost*. 2005;3(12):2730–2737.
64. Solini A, Chiozzi P, Morelli A, Fellin R, Di Virgilio F. Human primary fibroblasts in vitro express a purinergic P2X7 receptor coupled to ion fluxes, microvesicle formation and IL-6 release. *J Cell Sci*. 1999;112(pt 3):297–305.